Biochimica et Biophysica Acta 1787 (2009) 252–263

Contents lists available at ScienceDirect

Biochimica et Biophysica Acta

journal homepage: www.elsevier.com/locate/bbabio

Electron transfer protein complexes in the thylakoid membranes of heterocysts from the cyanobacterium *Nostoc punctiforme*

Tanai Cardona [a], Natalia Battchikova [b], Pengpeng Zhang [b], Karin Stensjö [a], Eva-Mari Aro [b], Peter Lindblad [a], Ann Magnuson [a,*]

[a] *Department of Photochemistry and Molecular Science, Ångström laboratory, Uppsala University, P.O. Box 523, SE-75120 Uppsala, Sweden*
[b] *Plant Physiology and Molecular Biology, Department of Biology, University of Turku, FIN-20014 Turku, Finland*

ARTICLE INFO

Article history:
Received 16 October 2008
Received in revised form 15 December 2008
Accepted 13 January 2009
Available online 30 January 2009

Keywords:
Cyanobacteria
Nostoc
Heterocyst
Photosystem II
Fluorescence
BN-PAGE

ABSTRACT

Filamentous, heterocystous cyanobacteria are capable of nitrogen fixation and photoautotrophic growth. Nitrogen fixation takes place in heterocysts that differentiate as a result of nitrogen starvation. Heterocysts uphold a microoxic environment to avoid inactivation of nitrogenase, e.g. by downregulation of oxygenic photosynthesis. The ATP and reductant requirement for the nitrogenase reaction is considered to depend on Photosystem I, but little is known about the organization of energy converting membrane proteins in heterocysts. We have investigated the membrane proteome of heterocysts from nitrogen fixing filaments of *Nostoc punctiforme* sp. PCC 73102, by 2D gel electrophoresis and mass spectrometry. The membrane proteome was found to be dominated by the Photosystem I and ATP-synthase complexes. We could identify a significant amount of assembled Photosystem II complexes containing the D1, D2, CP43, CP47 and PsbO proteins from these complexes. We could also measure light-driven in vitro electron transfer from Photosystem II in heterocyst thylakoid membranes. We did not find any partially disassembled Photosystem II complexes lacking the CP43 protein. Several subunits of the NDH-1 complex were also identified. The relative amount of NDH-1M complexes was found to be higher than NDH-1L complexes, which might suggest a role for this complex in cyclic electron transfer in the heterocysts of *Nostoc punctiforme*.

1. Introduction

Cyanobacteria are a diverse group of bacteria, capable of oxygenic photoautotrophic growth. By their ability to split water into oxygen and reductants, cyanobacteria prompted the development of higher plants ca half a billion years ago. Many cyanobacteria, such as the filamentous, heterocyst-forming cyanobacteria, have the capacity to fix atmospheric nitrogen into ammonia. *Nostoc punctiforme* PCC 73102 (identical to *Nostoc punctiforme* ATCC 29133, henceforth referred to as *Nostoc punctiforme*), is a filamentous cyanobacterium of symbiotic origin, able to express different phenotypes depending on environmental conditions [1]. When cultured under nitrogen-limiting conditions, 5–10% of the vegetative cells in the filament will differentiate into nitrogen fixing heterocysts [2–5].

Nitrogen fixation is carried out by the multimeric enzyme complex nitrogenase [6–8]. The nitrogenase active site contains a polynuclear Mo–Fe complex that is inactivated by oxygen [9–11]. Genes encoding the enzymes involved in nitrogen fixation are therefore only expressed after the oxygen level has dropped below a critical level, and the transcription of nitrogenase genes is stopped if the oxygen pressure is increased [10].

Oxygenic photosynthesis, which is the main source of ATP and reductants for the free-living organism, is diminished in the heterocysts, in order to keep the oxygen concentration at a minimum. The water oxidizing activity of Photosystem II (PSII) as well as fluorescence emission at 685 nm, associated with PSII, has been reported to be lacking in intact heterocysts from several filamentous strains [12,13]. It has been hypothesized that PSII activity is decreased due to the absence of phycobilisomes that are the main light-harvesting complexes for PSII in the vegetative cells [12,13]. The reaction centre proteins of PSII have been suggested to be degraded during heterocyst differentiation, although there have been some indications that PSII proteins can still be found in the mature heterocyst [14,15].

Aside from downregulation of photosynthesis, other mechanisms contribute to keeping a micro-oxic environment in the heterocysts; two extra envelope layers are constructed to reduce the permeability

Abbreviations: ATP, adenosine triphosphate; BN, blue native; Chl, chlorophyll; CLSM, confocal laser scanning microscopy; DM, *n*-dodecyl β-D-maltoside; DBMIB, dibromothymoquinone; DCBQ, 2,6-dichloro-*p*-benzoquinone; DCMU, 3-(3,4-dichlorophenyl)-1,1-dimethylurea; DCPIP, 2,6-dichlorophenolindophenol; DPC, diphenylcarbazide; EDTA, ethylene diamine tetraacetic acid; ESI, electrospray ionization; FNR, ferredoxin: NADP+ reductase; Hepes, 4-(2-hydroxyethyl)-1-piperazineethanesulfonic acid; Mes, 4-morpholinoethane-sulfonic acid; MS, mass spectrometry; NDH-1, NAD(P)H dehydrogenase; PAGE, polyacrylamide gel electrophoresis; PPBQ, phenyl-*p*-benzoquinone; PSI, Photosystem I; PSII, Photosystem II; Rubisco, Ribulose-1,5-bisphosphate carboxylase/oxygenase; SDS, sodium dodecyl sulfate; Tris, tris(hydroxymethyl)aminomethane; TOF, time of flight

* Corresponding author. Tel.: +46 18 4716582; fax: +46 18 4716844.
E-mail address: ann.magnuson@fotomol.uu.se (A. Magnuson).

0005-2728/$ – see front matter © 2009 Elsevier B.V. All rights reserved.
doi:10.1016/j.bbabio.2009.01.015

of O_2 into the heterocyst [16,17]. The discovery of heterocyst specific terminal oxidases in several filamentous strains supports the view that oxygen consumption is enhanced in heterocysts [18–20].

Nitrogen fixation is an energy demanding process, with a very high requirement of ATP and reducing equivalents. Since the heterocysts do not have water oxidation as primary source of reducing equivalents, it has been suggested that the reductants needed for nitrogen fixation are supplied via the pentose phosphate pathway [21,22], by carbon sources imported into the heterocysts from the vegetative cells [9,23]. The nitrogenase is probably directly reduced by heterocyst specific ferredoxins in *Anabaena variabilis* and *Anabaena/Nostoc* PCC 7120 [24,25]. Ferredoxin is assumed to be reduced by ferredoxin:NADP reductase (FNR) which has been found to be upregulated in heterocysts of *Anabaena sp.* and *Anabaena/Nostoc* PCC 7120 [26,27]. The main electron transfer route towards ferredoxin reduction in heterocysts is to a large extent unknown. Nitrogen fixation occurs at a higher rate under irradiation than in the dark, suggesting that Photosystem I (PSI), which remains active in heterocysts, plays an important role for the supply of ATP and/or reduced equivalents for nitrogen fixation [13,28–30].

In the vegetative cells, respiration and oxygenic photosynthesis take place in the same cellular compartment, but are segregated into different regions of the intracellular membrane system. While several respiratory enzymes are operative both in the thylakoid and cytoplasmic membranes, photosynthetic reaction centres appear primarily in the thylakoid membrane, whereas terminal oxidases seem confined to the plasma membrane [31,32]. In heterocysts, the intracellular membrane structure is different from vegetative cells, displaying e.g. a heterocyst-specific arrangement known as 'honeycomb' structures close to the cellular poles [33]. In addition to the electron transport pathways remaining unclear, the organization and composition of the energy converting membranes in heterocysts is still poorly understood.

In the present study we investigate the composition of membrane protein complexes in heterocyst membranes of *Nostoc punctiforme*. Recently, several groups have undertaken global proteomic investigations of this species, and with advances in quantitative shotgun proteomics our understanding of the nitrogen fixation process will be enhanced [34,35]. However, understanding the function of the membrane proteome requires analysis of both structure and function using techniques that are less detrimental for the assembled membrane protein complexes. Previously, analyses of membrane protein complexes of e.g. *Synechocystis* PCC 6803 and *Nostoc punctiforme* have revealed important aspects of the membrane protein composition, which are not reachable from a shotgun approach [36–38].

Here we present results from analyses of isolated membranes from the heterocysts of *Nostoc punctiforme*. The membrane protein complexes in the thylakoids were analyzed via 2D-gel electrophoresis and mass-spectrometry, and characterized by biophysical measurements. An interesting finding is that assembled PSII complexes are found in heterocysts, and that these complexes are capable of light-induced electron transfer.

2. Materials and methods

2.1. Culture conditions and isolation of heterocysts

The following protocol was developed based on methods described previously [26,28,39], with modifications as described below. Filaments of *Nostoc punctiforme* sp. strain PCC 73102 (from now on referred to as *Nostoc punctiforme*) were cultivated under nitrogen fixing conditions in $BG11_0$ medium: 1.5 l batch cultures to a total volume of 6 to 10 l were used and enriched with 3–5% CO_2, stirred and illuminated continuously with a light intensity of 30 $\mu E/m^2$ s. Approximately 7% of the cells differentiated into heterocysts as judged by light microscopy. The cultures were harvested during mid log phase after 7 days of growing (the chlorophyll-*a* content of the culture was 0.7 mg/l), by centrifugation at 5000 ×*g* for 10 min and resuspended immediately in Buffer solution A (Buffer solution A: 0.4 M sucrose; 50 mM Hepes/NaOH, pH 7.2; 10 mM NaCl; 10 mM EDTA), in a volume of ca 35 ml, at a chlorophyll-*a* (Chl-*a*) concentration of 150 μg/ml.

Prior to cell lysis, the cell suspension was incubated for 30 min at 4 °C in darkness. A freshly prepared solution of lysozyme from chicken egg white (Calbiochem) was added at a concentration of 1 mg/ml, and the suspension was incubated at 35 °C for 60 min in a shaker incubator in the dark. The cell suspension was sonicated on ice at full amplitude (27 W, Sonics Vibracell, VC-130). Sonication was done at intervals of 10 s. After each interval, the suspension was inspected in a light microscope. After a total sonication time of 1 min (6×10 s), only the heterocysts were left intact. The heterocysts retained their colour and cellular structures such as polar bodies after this treatment.

After sonication, the suspension was centrifuged at 1000 ×*g* for 5 min, and the supernatant, containing material from disrupted vegetative cells, was discarded. The pellet, containing the heterocysts, was manually homogenized using a Potter homogenizer pestle, and resuspended in Buffer solution A. The suspension was centrifuged at 500 ×*g* for 5 min, after which the supernatant was discarded. The pellet was again homogenized, resuspended in Buffer solution A, and centrifuged at 500 ×*g* for 5 min. Two additional washing steps were performed as above, with the only change that the *g*-force was reduced to 250 ×*g*, and the time to 3 min. The low speed and short centrifugation time was used during these last washing steps, to avoid co-sedimentation of membranes or cell wall debris from vegetative cells, together with the intact heterocysts. After the final centrifugation, the supernatant was discarded and the pellet was resuspended in Buffer solution A, to a final concentration of ca 0.5 mg Chl-*a* ml^{-1}. The suspension of isolated heterocysts was inspected by light and confocal laser scanning microscopy (see below), and stored at −80 °C.

A different batch culture of *Nostoc punctiforme* was later used as control for Western blot experiments (see below). That batch was grown as described above, but with additional supply of ammonia as nitrogen source.

2.2. Preparation of thylakoid membranes from heterocysts

The procedures described in this paragraph were performed in dim green light, and at 4 °C or on ice. Isolation of thylakoid membranes from the heterocysts was carried out by essentially the same protocol that we developed for thylakoid membrane isolation from vegetative cells [38], with modifications as follows: the suspension containing intact heterocysts at 0.5 mg Chl-*a* ml^{-1}, was mixed in a 1:1 ratio (v/v) with Buffer solution B (Buffer solution B: 0.8 M sucrose; 10 mM MES/NaOH, pH 6.35; 20 mM $MgCl_2$; 20 mM $CaCl_2$; 1 mM benzamidine; 1 mM phenylmethylsulfonyl-fluoride (PMSF)).

The suspension was placed in the sample chamber of a Parr cell disruption vessel (model 4639, Parr Instrument Company), and pressurized with N_2 to 170 bars. The high pressure was maintained for a minimum duration of 5 min, until the gas was homogenously distributed in the heterocysts. The suspension was then discharged through the sample outlet valve, at the bottom of the still pressurized sample chamber. The sudden depressurization led to lysis of the cells. The pressurization/depressurization procedure was done three times consecutively to the heterocyst suspension, to increase the yield of cell lysis.

The suspension was centrifuged at 5000 ×*g* for 5 min. After centrifugation, the supernatant, containing thylakoid membranes, was collected and kept on ice in the dark. The pellet, containing cell walls and the remaining intact heterocysts, was resuspended in Buffer solution B. The pressurization treatment was repeated as above for the resuspended pellet. After the last depressurization step, the suspension was centrifuged at 5000 ×*g* for 5 min. After the centrifugation, the supernatant was collected and kept on ice in the dark. The remaining

pellet was resuspended in Buffer solution B, given the same high-pressure treatment as before, and centrifuged at 5000 ×*g* for 5 min.

After the final centrifugation, the pellet contained cell walls and a fraction of thylakoid membranes still attached to the cell wall. This pellet (referred to below as the 'cell wall membrane fraction') was resuspended in Buffer solution C (Buffer solution C: 0.8 M Sucrose; 20 mM $CaCl_2$; 20 mM $MgCl_2$; 10 mM MES-NaOH, pH 6.35) at a concentration of 0.5 mg Chl-*a* ml^{-1} and stored at −80 °C.

The supernatant containing the thylakoid membranes was pooled together with the two previously collected supernatants, and the entire suspension (referred to below as the 'thylakoid membrane fraction') was centrifuged at 48,000 ×*g* for 60 min at 4 °C. The resulting supernatant after this step, contained mainly soluble proteins, and was discarded. The pellet, containing thylakoid membranes, was resuspended in Buffer solution C at 0.2 mg Chl-*a* ml^{-1}, and stored at −80 °C.

2.3. Determination of chlorophyll-a and protein content

Chl-*a* was extracted from the cells with 90% methanol. Absorbance was determined at 665 nm, and the Chl-*a* content was calculated with an extinction coefficient of 78.74 l g^{-1} cm^{-1} [40]. For gel electrophoresis and biophysical measurements, the protein content of thylakoid membranes and cell walls, was calculated according to the method of Bradford (595 nm) according to BioRad Protein Assay, Section 2 (BioRad).

2.4. Western blotting

Western blotting using antibodies against the Rubisco large subunit (RbcL) was used to control the purity of the heterocysts. The total protein content in samples of total cell extracts, was determined by using the BCA Protein assay (Pierce Biotechnology, Inc., Rockford, IL) with bovine serum albumin as a standard.

Protein samples (10 μg per lane) were separated by discontinuous SDS-PAGE [27] with a 12% resolving gel and a 3% stacking gel. After electrophoresis, proteins were either stained with Coomassie blue or transferred to Hybond ECL nitrocellulose membranes (Amersham Biosciences, Buckinghamshire, United Kingdom). Membranes were incubated for 1 h in 5% skim milk in Buffer solution D (Buffer solution D: 20 mM Tris–HCl pH 7.4, 140 mM NaCl, 0.05%–0.15% Tween), washed in the same buffer, and then incubated with anti-RbcL antibodies (Agrisera, Sweden) at a 1:10,000 dilution in a suspension of 2% skim milk in Buffer solution D (0.015% Tween). This was followed by washing in Buffer solution D and incubation with a horseradish-peroxidase-conjugated anti-rabbit antibody (BioRad) at a 1:5000 dilution. Immunodetection was visualized by chemoluminescence Western blotting ECL detection reagents (GE Healthcare, Sweden) on a ChemiDoc Imager (BioRad).

2.5. Confocal microscopy

Confocal laser scanning microscopy (CLSM) was performed with a Leica TCS-SP microscope with an inverted DMRIB stand. Exciting light at 488 nm was provided by an argon laser. Sample emission was collected at different wavelength ranges; in one channel emission was detected at 650–690 nm, to capture fluorescence from phycobilisomes and PSII. In a second channel emission was detected at 700–740 nm to capture mainly fluorescence from PSI. Fluorescence intensities of the vegetative cells and heterocysts, were analyzed from the digital images using the ImageJ 1.35 software (http://rsb.info.nih.gov/ij/, Wayne Rasband, National Institute of Health, USA). The fluorescence intensity varied between different locations within each cell. The total emission intensity from a given cell was therefore integrated over the cell image area and compared to that of cells from the same type (e.g. heterocysts). The average intensity per cell was obtained from three independently sampled images. For visualizing the distribution between different emission wavelengths, the images from the two confocal channels were coloured green or red using Adobe® Photoshop® 7.0, for the short and long wavelength emission bands respectively.

2.6. Oxygen evolution and electron transfer measurements

Oxygen evolution by PSII was assayed at 25 °C using a Clark-type oxygen electrode (Hansatech, UK). Saturating illumination was provided with 150 W slide projector lamp, equipped with an orange long-pass filter that has no transmittance at wavelengths below 570 nm (OG590, Schott Glass Technologies Inc.). Oxygen evolution of thylakoid membranes and intact cells was measured using 2 mM $K_3[Fe(CN)_6]$ and 1 mM 2,6-dichloro-*p*-benzoquinone (DCBQ), or 1 mM phenyl-*p*-benzoquinone (PPBQ) as electron acceptors. The thylakoid suspension was diluted in the measuring solution to a chlorophyll concentration of 20 μg Chl-*a* ml^{-1}.

Electron transfer through PSII was assayed by measuring the light-driven reduction of the artificial electron acceptor 2,6-dichlorophenolindophenol (DCPIP) using the artificial electron donor diphenylcarbazide (DPC). DPC acts as electron donor to Tyrosine-Z in the absence of an intact water oxidizing manganese complex [41]. The thylakoid suspension was diluted in the thylakoid buffer solution (see above) to a Chl-*a* concentration of 20 μg Chl-*a* ml^{-1}. 0.1 mM DCPIP was added to the suspension in the dark, and 1 μM dibromothymoquinone (DBMIB) was added to prevent unwanted oxidation of the reduced electron acceptor by the Cytochrome b_6/f complex. Reduction of DCPIP in the presence or absence of 0.5 mM DPC, was measured using a Shimadzu UV-3000 dual wavelength/double beam recording spectrophotometer. The reduction can be followed by measuring the change in absorbance difference ($\Delta\Delta A$) between 530 nm and 570 nm, as a function of time during illumination of the sample. Sideways illumination was provided with a 150 W slide projector lamp with a 590 nm cut-off filter. In additional measurements, 20 μM of the PSII specific inhibitor (3,4-dichlorophenyl)-1,1-dimethylurea (DCMU) was added to verify that the observed reduction of DCPIP was a product of electron transport through PSII.

2.7. Fluorescence emission spectroscopy

Fluorescence emission spectra from intact filaments, intact heterocysts, and thylakoid membranes from vegetative cells and from heterocyst cells, were recorded at 77 K on a Spex Fluoromax 2 spectrometer (Jobin Yvon Ltd., UK). Excitation was made at 427 nm and 570 nm respectively, using a slit width of 1 nm. All samples were diluted to 10 μg Chl-*a* ml^{-1} in 88% glycerol.

2.8. Determination of Mn concentration by electron paramagnetic resonance spectroscopy

The Mn content of intact filaments and heterocysts was determined essentially as in [38]. Briefly: samples of isolated heterocysts and intact filaments respectively, were washed in Buffer A (see above), with the addition of 10 mM EDTA to chelate all extracellular Mn. The cells were centrifuged shortly and resuspended in a solution containing 0.2 M HNO_3 and 0.1 M $CaCl_2$, to denature all membranes and proteins, and release all Mn. The samples were incubated for 30 min, and centrifuged at 15,000 ×*g*. The intensity of the hexaquo-Mn(II) EPR signal was measured on the supernatant, at room temperature. A standard curve based on the line intensities of $MnCl_2$ solutions was used for quantification.

2.9. 2D blue native/SDS-PAGE

The thylakoids were solubilized at a protein concentration of 10 μg/μl in either 1.5, or 2% w/v *n*-dodecyl β-D-maltoside (DM) followed by BN/PAGE. 2D BN/SDS-PAGE was performed as follows: the thylakoid membranes were washed with 330 mM sorbitol, 50 mM BisTris (pH

7.0) buffer, and 250 μg ml^{-1} Pefabloc (Roche Diagnostics, Indianapolis); centrifuged at 18,000 ×g for 10 min and resuspended in 20% w/v glycerol, 25 mm BisTris (pH 7.0), 10 mM $MgCl_2$, 0.1 U μl^{-1} RQ1 RNAse-Free DNAse (Promega, Southampton, UK), and 250 μg ml^{-1} Pefabloc at a protein concentration of 20 μg/ml. An equal volume of buffer containing 4.0% w/v DM (Sigma) was added under continuous mixing and was allowed to incubate for 20 min on ice, followed by 10 min at room temperature. The insoluble fraction was separated from the soluble fraction by centrifugation at 18,000 ×g for 20 min. The supernatant was mixed with 0.1 volumes of Coomassie blue solution (5% w/v Serva blue G, 100 mM BisTris, pH 7.0, 30% w/v sucrose, 500 mM ε-amino-*n*-caproic acid, and 10 mM EDTA). This sample solution was loaded over a 0.75 mm thick, 5% to 12.5% w/v acrylamide gradient gel (Hoefer Mighty Small mini-vertical unit, Amersham Pharmacia Biotech, Uppsala) containing 500 mM ε-amino-*n*-caproic acid. Electrophoresis was performed at 4 °C by increasing voltage from 50 to 200 V during a 6 h run. Once finished, the lanes were excised and incubated in SDS sample buffer containing 7% v/v β-mercaptoethanol and 6 M urea for 1 h at room temperature; layered on a 1 mm thick SDS polyacrylamide gel [42], with 14% w/v acrylamide and 6 M urea in the separating gel. The proteins were visualized by silver staining [43].

2.10. Identification of proteins by mass spectrometry

Silver-stained protein spots were excised from a dry SDS polyacrylamide gel and saturated with 100 mM ammonium bicarbonate. The proteins were 'in-gel' reduced, alkylated and digested with Trypsin Gold (Promega, USA) according to [44]. After digestion, the peptides were eluted by washing of the gel pieces for 1 h, consecutively with 5% formic acid, 5% formic acid/50% acetonitrile, and 5% formic acid/80% acetonitrile. The extracts were combined and dried in a Speedvac.

Tandem mass spectrometry was performed on a API QSTAR spectrometer (Applied Biosystems, Foster City, USA) equipped with a Nano electrospray source (Protana, Toronto, Canada) and connected in-line with the nano HPLC system and the auto sampler (LC Packings, Amsterdam, Netherlands). Eluted and dried protein digests were dissolved in 10 μl of 2% formic acid, centrifuged for 10 min at 12,000 ×*g*, and transferred into an auto sampler vial. Aliquots (8 μl) of samples were loaded onto a C18 PepMap, 5 μm, 5 mm × 300 μm I.D. nano-precolumn (LC Packing, Amsterdam, Netherlands), desalted for 4 min and subjected to reverse-phase chromatography on a C18 PepMap, 3 μm, 15 cm × 75 μm I.D. nanoscale LC column (LC Packing, Amsterdam, Netherlands). A gradient of 2–50% acetonitrile in 0.1% formic acid was applied for 30 min using a flow rate of 0.2 μl/min.

The acquisition of MS/MS data was performed on-line using the fully automated IDA feature of the Analyst QS software (Applied Biosystems, Foster City, USA). The acquisition parameters were 1 s for TOF MS survey scans, and 2 s for the product ion scans of the two most intensive doubly or triply charged peptides. Analyses of MS/MS data were performed with the Analyst QS software followed by protein identification by Mascot, with search parameters allowing for carbamidomethylation of cystein, one miscleavage of trypsin, oxidation of methionine, mass accuracy of 0.2 Da for precursor peptides and of 0.3 Da for ions in MS/MS spectra. The NCBI database was used for protein identification. One of the proteins (*ndhI* gene product) was identified as a hypothetical protein in the NCBI database. However, by homology to other cyanobacterial sequences it could be clearly identified as the NdhI protein.

3. Results and discussion

3.1. Isolation of intact heterocysts from filaments

In a previous study we developed a preparation protocol for isolating the thylakoid membrane fraction in vegetative cells of *Nostoc punctiforme*, with the objective to expand this protocol to the isolation of membrane fractions from heterocysts [38]. To achieve a reliable proteomic analysis of the thylakoid membranes in heterocysts, we wanted to ascertain a high purity of the preparation. Two different types of contamination from vegetative cells may occur: by unbroken filaments or intact single vegetative cells, and by debris of ruptured vegetative cells and their thylakoid membranes. Due to the difference in toughness of the cell wall of the vegetative cells and heterocysts, vegetative cells can be disrupted by sonication, while the heterocysts are left intact.

To isolate the heterocysts, the culture was treated with lysozyme, after which the vegetative cells were broken via mild sonication. To verify that no filaments or intact vegetative cells remained after sonication, the cells were carefully inspected by light microscopy. The heterocysts were left intact and retained all major structural components such as polar bodies, after this treatment. We used heterocyst specific staining by Alcian blue (as described by Liu and Golden [45]) to investigate if the outer envelope had been damaged by the treatment. The isolated heterocysts were stained to the same degree as heterocysts in intact filaments, indicating that the outer envelope was intact (not shown).

Contamination by cell debris and membranes from ruptured vegetative cells was minimized by several centrifugation steps followed by careful homogenization. To avoid precipitation of lighter cell fragments, the centrifugation speed was successively reduced. The cell suspension was inspected again by light microscopy after all centrifugations. We thereby achieved a heterocyst preparation of high purity, and the final supernatant was clear and uncoloured.

3.2. Confocal laser scanning microscopy (CLSM)

In filamentous cyanobacteria, the phycobilisomes are degraded during nitrogen starvation and early onset of heterocyst differentiation, leading to a lower intensity of auto fluorescence from the proheterocysts and heterocysts, compared to the vegetative cells [45–47]. We utilized CLSM to characterize the purity of the heterocyst preparation. Fig. 1 shows the combined images from both confocal channels, after artificial colouring was added for clarity: Images of cells emitting in the shorter wavelength interval (650–690 nm) was coloured green, and images of cells emitting in the longer wavelength interval (700–740 nm) was coloured red. Cells that exhibit fluorescence in both intervals therefore display a variety of yellow and orange shades.

Fig. 1A shows whole filaments that have grown under nitrogen fixing conditions for 7 days. The vegetative cells in the filaments were strongly fluorescent in the 650–690 nm range, and also displayed low intensity fluorescence in the 700–740 nm range. The high intensity in the shorter wavelength interval reflects that fluorescence in the vegetative cells mainly originates from phycobilisomes at ca 650–660 nm.

The heterocysts displayed weaker emission intensity over the entire spectral range (at arrows in Fig. 1A). Emission from 650 to 740 nm, with emphasis on the longer ('red') wavelengths, was detected from heterocysts in filaments, and was clearly seen after maximizing the photomultiplier sensitivity. Emission from remaining phycobiliproteins in the heterocysts could also be detected (see 77 K fluorescence spectroscopy section below). However, the emission intensity from the phycobiliproteins was much lower in the heterocysts than in the vegetative cells, consistent with lower phycobilisome content.

After the heterocysts were isolated from the filaments, the emission spectrum changed somewhat. Fig. 1B and C display the purified heterocysts after the final washing steps. It can be seen that the heterocysts were emitting to a varying degree within the wavelength range from 650 to 740 nm, resulting in the yellow and orange colour tones of the heterocyst images (Fig. 1B). The spectral change in the heterocysts after isolation could be attributed to a higher degree of quenching of the long-wavelength fluorescence from

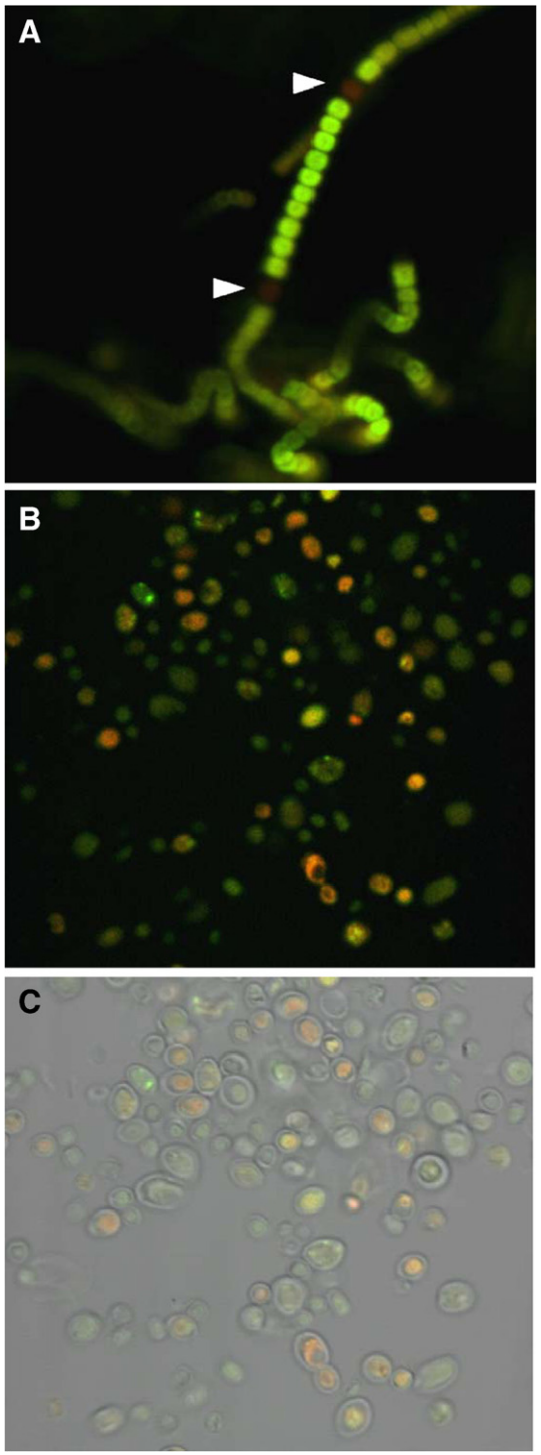

Fig. 1. Laser-scanning confocal microscopy pictures taken in a single plane. (A) Nitrogen fixing filaments magnified 1000×, white arrows indicate heterocysts along the filament. (B) depicts isolated heterocysts obtained by sonication of whole filaments. The detector sensitivity was increased by 25% compared to the picture in A, in order to enhance fluorescence detection. (C) depicts an image taken in transmission mode, superimposed on the confocal image in B. In C the thick cell walls characteristic of heterocysts can be observed.

PSI. In isolated heterocysts, the redox balance is disturbed due to interrupted supply of electron donors from the vegetative cells, or perhaps by leakage of electron carriers from the heterocysts. During sample preparation for confocal microscopy, the primary donor P_{700} became oxidized in a portion of PSI centres, leading to quenching of the fluorescence at 720 nm and redirecting the excitation energy to remaining phycobiliproteins (see 77 K fluorescence spectroscopy section below). Therefore the emission spectrum in isolated heterocysts was shifted towards shorter wavelengths compared to the heterocysts in intact filaments. The presence of a stable P^{+}_{700} in the isolated heterocysts, which had been kept at room temperature, was confirmed by EPR spectroscopy (not shown).

From our observations of fluorescence emission in heterocysts from both filaments and isolated heterocysts, it is clear that some phycobiliproteins remain in the mature heterocysts. To compare the emission intensity in vegetative cells and heterocysts, we used image analysis software. Images from each confocal channel were analyzed separately. The average emission intensity from heterocysts was found to be 20–25 times less than in vegetative cells, over the entire spectral range. In all of the isolated heterocysts, the average emission intensity was the same as in the heterocysts in the intact filaments. Therefore we conclude that our isolated heterocyst preparation contained no contaminating intact vegetative cells, since these would have been noticed by their significantly higher emission from the phycobilisomes.

3.3. 77 K fluorescence spectroscopy

The images of isolated heterocysts collected by CLSM, indicated that some phycobiliproteins remained in the heterocysts, despite the

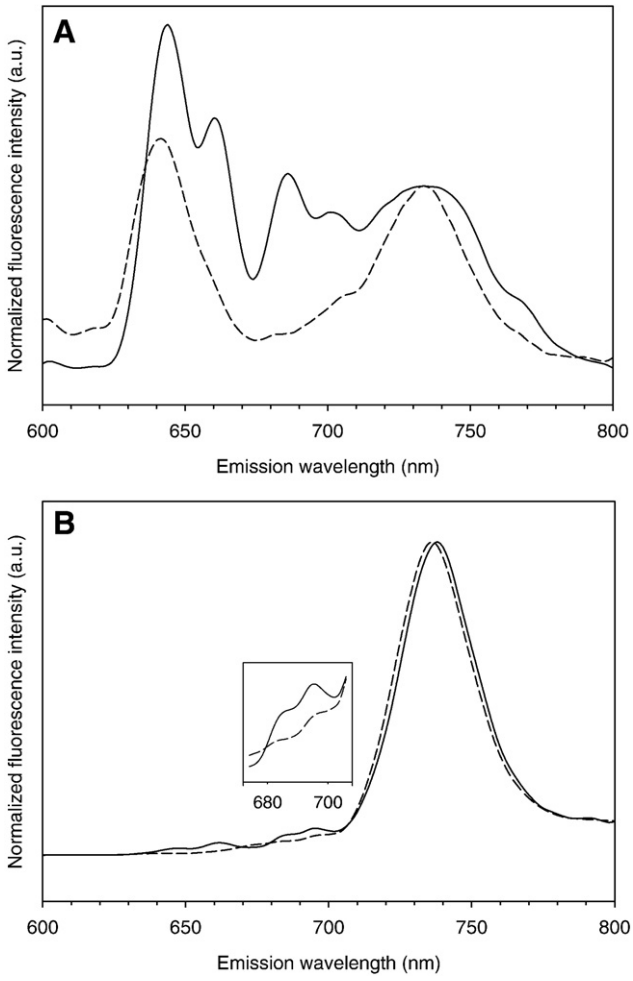

Fig. 2. Fluorescence emission spectra at 77 K from vegetative cells and heterocysts of *Nostoc punctiforme*, at different excitation wavelengths. Spectra from intact filaments (—) and heterocysts (- -) after excitation at 570 nm (A) and 427 nm (B). The insert in B shows an enlargement (5×) of the two spectra, enhancing the peaks at 685 and 695 nm originating from PSII. All samples were adjusted to the same Chl-*a* concentration prior to measurement, and the spectra were pair wise normalized to the emission intensity at the maximum emission from PSI (approx. at 730 nm).

degradation of the phycobilisomes which follows on heterocyst differentiation. PSI contains a Chl-*a* antenna of ca 90–95 Chl-*a* molecules per reaction centre [49], but an auxiliary antenna would presumably make photophosphorylation in heterocysts more efficient. To investigate this option we measured the fluorescence emission from whole filaments and isolated heterocysts at 77 K.

Fig. 2 shows normalized fluorescence emission spectra collected from whole filaments and isolated heterocysts. Excitation was made at 570 nm (Fig. 2A) and 427 nm (Fig. 2B). In the intact filaments, emission from the phycobilisomes and PSII is most noticeable after excitation at 570 nm (Fig. 2A, solid line). The peaks at 643 and 660 nm arise from phycocyanin and allophycocyanin respectively, and the peaks at 685 and 695 nm originate from the PSII reaction centre [48,50,51].

When Chl-*a* specific excitation was chosen we observed emission bands from PSII at 685 and 695 nm in both vegetative cells and in heterocysts (Fig. 2B). The emission from PSII was lower but still noticeable in the heterocysts, indicating that the mature heterocysts contained PSII complexes (Fig. 2B, insert). This was confirmed by our analysis of the protein complex composition and electron transport in the heterocyst thylakoid membranes that are shown and further discussed below.

The peak at 738 nm stems from Chl-*a* molecules in the PSI reaction centre pigments, and is most prominent when Chl-*a* specific excitation is chosen (Fig. 2B). The higher intensity of fluorescence from PSI [51] compared to fluorescence intensity from PSII can be attributed to a higher PSI to PSII ratio in the thylakoid membranes (about 3–4 in vegetative cells [38]).

Emission from PSI was observed under Chl-*a* specific excitation in both filaments and heterocysts, but the emission from PSI was substantial also when the phycobilisome absorption band was excited. In the heterocysts, the phycobilisome spectrum was dominated by emission at 640 nm (Fig. 2A, dashed line). However, there was also considerable emission from PSI, indicating that phycocyanin can contribute to energy transfer to PSI in the heterocyst, in accordance with previous observations in heterocysts from *Anabaena variabilis* [50].

To explore the possible energy transfer from phycobilisomes or phycobiliproteins to PSI, we recorded excitation spectra from whole filaments and heterocysts at the 730 emission peak. The result is shown in Fig. 3. PSI fluorescence is most notably induced at the Chl-*a* absorption bands around 430 and 675 nm respectively. In the filaments, there are also prominent contributions at 570 nm (from phycoerythrin) and 620 nm (from phycocyanin), that overlap with the excitation bands of Chl-*a*. In the isolated heterocysts, the bands between 550 and 650 nm are diminished but still noticeable. The intensity of the peak at 620 nm was reduced to ca 40% in heterocysts, compared to that of filaments.

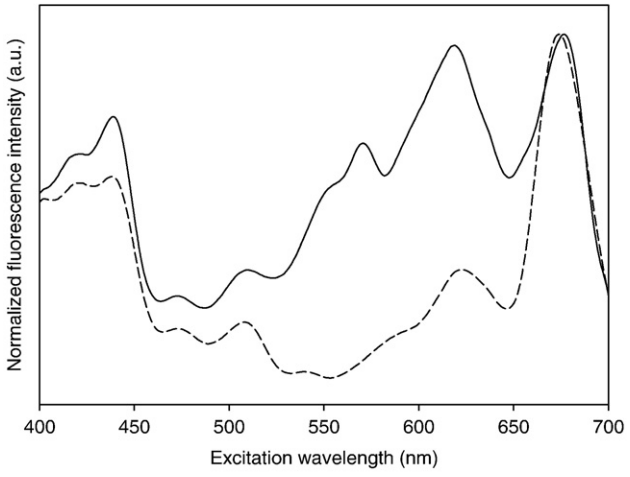

Fig. 3. Fluorescence excitation spectra at 77 K from vegetative cells (—) and heterocysts (- -), measured at 730 nm. The spectra were normalized to the maximum emission peak at 675 nm.

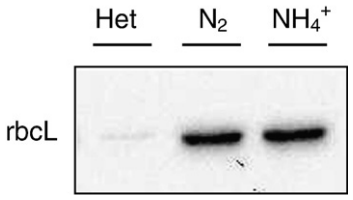

Fig. 4. Western blot demonstrating the amount of Rubisco in isolated heterocysts (Het), nitrogen fixing whole filaments (N_2) and filaments grown with ammonia (NH_4^+).

We conclude that although phycobilisome absorption and emission are clearly reduced in the heterocysts, there are still contributions by phycobiliprotein-associated excitation transfer to PSI. It has been proposed that changes in antenna coupling (so-called state transitions) involve movement of the entire phycobilisome from PSII to PSI or vice versa [52], but excitation transfer could also depend on direct contact between the photosystems [53,54]. An alternative explanation is that energy transfer can take place directly from phycocyanin rods to PSI, circumventing PSII altogether [55]. Our emission spectra from heterocyst clearly indicate that phycocyanin could act as an auxiliary antenna to PSI in heterocysts of *Nostoc punctiforme*. This supports earlier suggestions that energy transfer takes place between phycobilisomes and PSI. Association and energy transfer between phycocyanin and PSI was recently shown by Kondo et al., who suggested that core-less phycobilisomes are a naturally occurring antenna type, accountable for environmental adaptation in *Synechocystis* PCC 6803 [56].

3.4. Western blotting

To test the heterocyst preparation for contamination by vegetative cell contents, we measured the amount of ribulose-1,5-bisphosphate carboxylase/oxygenase (Rubisco). Rubisco is only expressed in vegetative cells, and the protein should therefore not be present at all in the heterocyst preparation [9,57]. In isolated thylakoid membranes from vegetative cells, we previously found a large amount of Rubisco, which co-purified with the thylakoid membranes [38]. If the isolated heterocysts had been contaminated by proteins from vegetative cells, Rubisco would be one contaminant that would be easy to detect.

We performed a Western blot analysis using an antibody raised against the Rubisco large subunit, RbcL. A comparison between isolated heterocysts, nitrogen fixing whole filaments, and filaments grown in a medium supplied with compound nitrogen, is shown in Fig. 4. The relative signal obtained from heterocysts on a total protein basis, was found to correspond to 4–7% of that in filaments. A realistic interpretation of this result is that the purity of the heterocyst preparation was ≥93–97%. To further validate the purity of the preparation we performed electron transfer experiments (see below).

3.5. Isolation of thylakoid membranes from heterocysts

We isolated thylakoid membranes from the purified heterocysts, by modifying our protocol for the isolation of thylakoids from filaments of *Nostoc punctiforme* [38]. To rupture the cells and obtain the thylakoid membranes, we used nitrogen pressurization and decompression. This resulted in a higher yield and better reproducibility than using glass beads or a French press (not shown). For heterocysts, it was necessary to pressurize the sample five times to achieve complete breakage of the cells.

After disruption of the heterocysts, the samples were divided into two fractions: a light fraction, containing pure thylakoid membranes, and a heavy fraction, containing cell walls, plasma membranes, and some thylakoid membranes. The heavy fraction will henceforth be referred to as the 'cell-wall membrane' fraction.

The yield of heterocyst thylakoid membranes was calculated on a chlorophyll-*a* (Chl-*a*) basis. The total Chl-*a* content in a typical batch culture of 6 l was ca 6.5 mg, and almost 10% of that, 0.6 mg, was found in the isolated heterocysts. After isolation, only ca 10.5% of the total amount of Chl-*a*, and 7.5% of the total membrane proteins in the heterocysts, were collected in the thylakoid membrane fraction. The remaining 89.5% of the Chl-*a,* and 92.5% of the membrane proteins, were found in the cell-wall membrane fraction. This was due to a tendency for the thylakoid membranes to 'stick' to the cell walls in heterocysts, maybe connected to the sub cellular 'honeycomb' structures that can be observed at the heterocyst poles. We chose not to try to increase the yield of purified thylakoid membranes by using e.g. sonication or detergents, as this might damage the supramolecular structures of membrane protein complexes.

However, the chlorophyll:protein ratio was on average 38% higher in the heterocyst thylakoid membrane fraction compared to the cell-wall fraction. This is an important result and shows that the membrane proteins in the isolated thylakoid fraction consisted mainly of the photosynthetic apparatus, whereas the membranes in the cell-wall fraction contained less photosynthetic proteins on a total protein basis.

3.6. Protein composition of isolated thylakoids and cell wall-associated membranes

In a previous study, we analyzed the membrane proteome of the isolated thylakoids from vegetative cells, by 2-dimensional gel electrophoresis and mass spectrometry. We then identified 28 individual proteins, including photosynthetic reaction centre proteins, ATP synthase subunits, and proteins from the Cytochrome-b_6/f complex [38].

Here we have analyzed the membrane protein complexes, in the isolated thylakoid membranes and the cell-wall membrane fraction from heterocysts. A mild solubilization of the membranes with dodecyl β-D-maltoside, allows intact membrane protein complexes to be separated in a blue-native (BN) gel (1st dimension). Individual subunits of each complex were then separated on a denaturing SDS gel (2nd dimension). The BN gels and the SDS gels, of thylakoid membranes and cell-wall membranes respectively, are shown in Fig. 5. The proteins were then identified by ESI–MS/MS. The results from protein identification are displayed in Table 1.

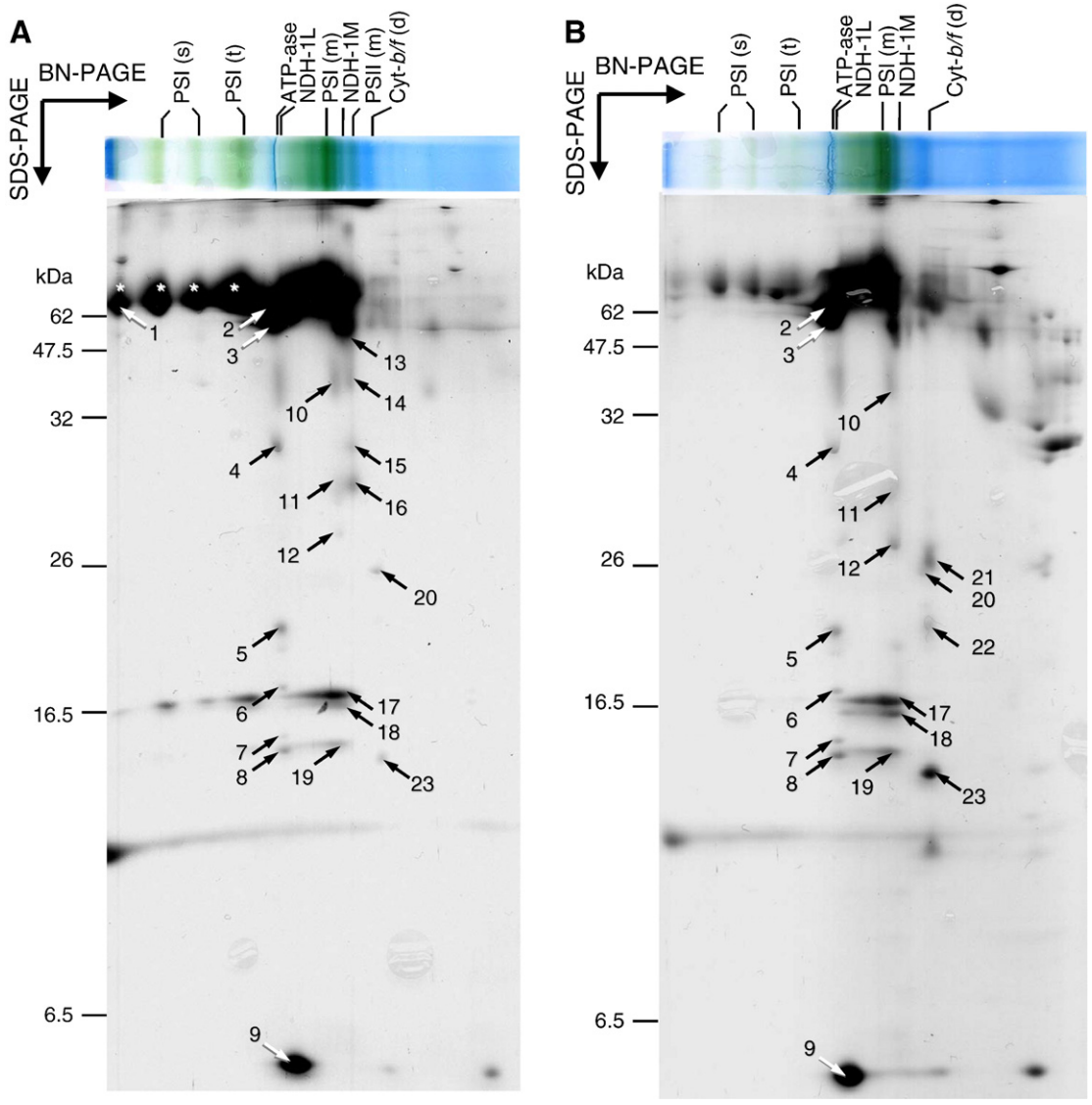

Fig. 5. Two-dimensional gel electrophoresis of membranes from heterocysts *Nostoc punctiforme*. (A) Purified thylakoid membranes, containing the bulk of photosynthetic proteins. (B) Membranes belonging to the cell wall fraction (see text for discussion). The upper gel lane is a blue-native (BN) gel where membrane protein complexes have been separated in their native form. The different forms of membrane protein complexes are: PSI(s) = super complexes of PSI, PSI(t) = trimers of PSI, PSI(m) = monomers of PSI, PSII(m) = monomers of PSII, NDH-1L = the large complex of NDH-1, NDH-1M = the medium-sized complex of NDH-1. The complexes in the BN gel were separated into the two-dimensional SDS-PAGE gel, and stained by silver staining. Selected proteins in the SDS-gel were excised and identified by MALDI-TOF mass spectrometry. The identified proteins are listed in Table 1 using the same numbering.

Table 1
Thylakoid membrane proteins in the heterocysts of *Nostoc punctiforme* sp. PCC 73102 identified by mass spectrometry

Spot no	Protein ID	Subject gene	NCBI accession number	Theor protein mass (kDa)	Identification by ESI–MS/MS	
					Peptides	Mascot score
1[a]	PSI core protein	*psaA*	gi:186683949	83.5	10	542
	PSI core protein	*psaB*	gi:186683950	83.3	8	399
	ATP-dependent Zn-protease	*ftsH*	gi:186684974	67.2	12	517
2	ATP synthase subunit α	*atpA*	gi:186684957	54.5	13	397
3	ATP synthase subunit β	*atpB*	gi:186684534	51.8	23	1998
4	ATP synthase subunit γ	*atpC*	gi:186684958	35.2	18	951
5	ATP synthase subunit b	*atpF*	gi:186684955	20.4	9	608
6	ATP synthase subunit δ	*atpD*	gi:186684956	20.4	11	621
7	ATP synthase subunit b'	*atpG*	gi:186684954	16.2	12	890
8	ATP synthase subunit ε	*atpE*	gi:186684533	14.7	6	387
9	ATP synthase subunit c	*atpH*	gi:186684953	8.1	3	567
10	NDH-1 subunit 7	*ndhH*	gi:186685062	45.4	8	454
11	NDH-1 20 kDa subunit	*ndhK*	gi:186685599	27.6	12	620
12	NDH-1 subunit I	*ndhI*[b]	gi:53686996	(9.6)	5	274
13	PSII protein: CP47	*psbB*	gi:186682779	56.4	7	254
14	PSII protein: CP43	*psbC*	gi:186683773	50.5	11	571
15[a]	PSII protein: D2	*psbD*	gi:186683774	39.3	5	307
	PSII protein: OEC33	*psbO*	gi:186684906	30.2	8	462
16	PSII protein: D1	*psbA*	gi:186685509	39.8	7	346
17	PSI extrinsic subunit D	*psaD*	gi:186685227	15.6	16	969
18	PSI reaction centre subunit XI	*psaL*	gi:186683995	18.3	8	415
19	PSI reaction centre subunit III	*psaF*	gi:186683993	18.2	6	393
20	Ferredoxin-NADP+-reductase	*petH*	gi:186683035	48.6	12	526
21	Cytochrome *f*	*petA*	gi:186680678	36.2	9	584
22	Cytochrome b_6	*petB*	gi:186680843	24.4	4	187
23	Cyt-b_6/*f* subunit IV	*petD*	gi:186680843	17.4	3	97

The numbering corresponds to the BN/SDS-PAGE gel in Fig. 5. Results of protein identification are presented as: an accession number of the protein in the NCBI database, a theoretical mass of the unprocessed protein, an amount of matched peptide masses that provided the protein identity, and a score value according to Mascot.

[a] Proteins of similar apparent molecular weight belonging to the same membrane protein complex, that were not resolved in the SDS gel and where found in the same sample.

[b] Sequence is annotated as 'hypothetical protein' for *Nostoc punctiforme*. Identification could be made by homology to protein sequences in other cyanobacteria (93% identity in *Anabaena variabilis*).

3.6.1. Photosystem II complexes

A most interesting result which we did not expect, was the finding of monomeric PSII complexes in the heterocyst thylakoid membranes (Fig. 5A). We identified the PSII reaction centre subunits CP47, CP43, D2, and D1 from these complexes (Table 1). Within the same stained area on the gel where the D2 protein was found, we also identified the PsbO, or extrinsic Mn-stabilizing protein, normally associated to PSII complexes active in water oxidation. This is a most surprising result since the main function of the PsbO protein is assumed to be stabilization of the water oxidizing complex. The lack of oxygen evolution from the heterocyst preparation (see below) would otherwise lead us to assume that all extrinsic PSII protein subunits are absent. With the PsbO still associated to the PSII complexes, there is less to suggest that PSII is completely inactivated in the heterocyst, and if it is, the mechanism is probably on the electron acceptor side.

We would like to stress the fact that the first dimension in the 2D gels was obtained by separation of intact protein complexes by size, in the non-denaturing BN gel. This is essential to our findings, since it means that the identified PSII subunits are all part of assembled PSII complexes, as opposed to disconnected individual subunits. A few individual PSII protein subunits have been found in heterocysts in earlier studies [14,15,29,47,58]. However, the presence of separate proteins shows no indication as to whether these proteins are part of assembled protein complexes, or leftovers from protein complex disassembly. To our knowledge, this is the first time that intact PSII complexes have been observed in heterocyst membranes.

We did not observe any PSII proteins at all in the membranes from the cell-wall fraction, where the respiratory enzymes were more abundant. This important observation suggests that the PSII complexes were a true constituent of the heterocyst thylakoids and not a contamination. There have so far been no reports that deal with the details of PSII inactivation during heterocyst differentiation. Disassembly and repair of PSII is known to take place in all oxygenic photosynthetic organisms due to light-induced damage to the D1 protein in the reaction centre core [59–61]. The repair cycle runs continuously in the light and starts with D1-degradation by specific proteases, followed by detachment of the extrinsic proteins and partial disassembly of the reaction centre core. Such partially disassembled PSII centres have been shown to lack the CP43 protein, but contain most other core transmembrane subunits [59].

Our heterocyst preparation contains monomeric PSII complexes that have at least the D1, D2, CP43, CP47, and PsbO proteins. We did not find any PSII complexes lacking the CP43 protein, or any other partly degraded PSII complexes. Our interpretation is that the PSII complexes observed in the heterocysts were not degradation products.

We then measured light-induced electron transport through PSII in the heterocyst membranes, in the presence of exogenous electron acceptor DCPIP (see below).

3.6.2. Photosystem I and ATP synthase complexes and proteins

The 2D gels were completely dominated by the intense staining of the PSI and ATP synthase proteins (Fig. 5A). The reaction centre proteins PsaA and PsaB were found within the same stained area and could be identified by ESI–MS/MS (Fig. 5A, spot number 1). We could observe several bands (marked with * in Fig. 5) of the same mass as the PsaA/B spot in the SDS gel, originating from complexes of higher molecular weight in the BN gel. These are larger multimeric forms of PSI complexes. In addition, we identified three low-molecular mass proteins; PsaD, PsaL and PsaF, from the monomeric PSI complexes.

Although silver staining has a poor linear range for absolute quantification of proteins, we can still compare the relative staining of several of the different complexes within the same gel, and by comparison with thylakoid membranes in the vegetative cells. In the heterocyst gels, the PSI and ATP synthase proteins stained very heavily, whereas other proteins, such as those from the NDH-1 and Cytochrome-b_6/*f* complexes, were only relatively faintly stained (Fig. 5). In the gels from vegetative cell thylakoids on the other hand, the staining was more even between the different protein complexes [38].

This indicates that the heterocyst thylakoids contain a much larger relative amount of PSI and ATP synthase complexes, than the vegetative cell thylakoids. The massive staining from PSI and ATP synthase in our gels, corroborates previous findings that these complexes are needed in very large amounts to generate enough ATP for nitrogen fixation [9,62], which is the basis for the upregulation of PSI proteins in heterocysts of *Anabaena/Nostoc* PCC 7120 [27,63].

Within the same area the PsaA and PsaB proteins we also found a protein which is homologous to the Zn-dependent protease FtsH. FtsH has been found in plant chloroplasts as well as in cyanobacteria, and is known to participate in a number of degradation processes, e.g. of the PSII D1 protein during light stress, as well as in biogenesis of several photosynthetic proteins [64]. This is the first time an FtsH homologue has been found in heterocysts of *Nostoc punctiforme*. Its location in the PsaA/PsaB complex seems to corroborate earlier findings that FtsH is essential for the assembly of functional PSI complexes in *Synechocystis* PCC 6803 [65].

3.6.3. Proteins from the Cytochrome-b_6/*f* complex

In contrast to the thylakoid membranes, the cell-wall membrane fraction displayed a markedly stronger staining of the proteins from the Cytochrome-b_6/*f* and NDH-1 complexes, while the high molecular weight PSI proteins stained rather weakly. Moreover, we could not observe any PSII complexes in the cell wall associated membranes. This suggests that the cell wall associated membranes are dominated by respiratory enzymes, whereas the photosynthetic proteins are in lower abundance compared to the isolated thylakoids, similar to what has been observed in other cyanobacteria [31,32]. The Cytochrome b_6/*f* complex is known to participate in PSI-driven cyclic electron transport [66,67], but is not restricted to the photosynthetic electron transport chain. It has been implied to function in respiratory electron transport as well [31,32,66].

We identified several subunits from the NDH-1 and Cytochrome-b_6/*f* protein complexes in the cell-wall membrane fraction (spots 21–23 in Fig. 5B) while they were difficult to identify in the thylakoid membranes due to their lower abundance in that fraction. From the dimeric Cytochrome-b_6/*f* complex we could identify the apocytochrome-*f* (PetA) subunit by mass-spectrometry. In the same row, we observed two more proteins belonging to the same protein complex. By comparison with vegetative cell thylakoids it can be concluded that these proteins are the Cytochrome-b_6 (PetB) and the subunit IV (PetD) in the Cytochrome-b_6/*f*-complex respectively [38]. The monomeric form of the Cytochrome-b_6/*f* complex was not discernible in the heterocysts, suggesting that it is either not present or only present in very low amounts.

In the cell-wall membrane fraction, we also identified the ferredoxin:NADP-reductase (FNR) which participates in cyclic electron transfer between PSI and the Cytochrome-b_6/*f*-complex [66–68]. The position of this protein spot in the gel was very close to the proteins of the Cytochrome-b_6/*f*-complex, but was clearly shifted as compared to the Cytochrome-b_6/*f* subunits. Although the FNR migrates close to the Cytochrome-b_6/*f*-complex, its off-centre position shows that it is clearly not a part of that complex.

3.6.4. Proteins and organization of the NDH-1 complex

The NDH-1 complex is a multi-subunit, proton translocating NAD(P)H:quinone oxidoreductase (reviewed in [69]). In *Synechocystis* PCC 6803, this enzyme occurs as one or three complexes of different composition; NDH-1L (large) and the smaller NDH-1M (medium) and NDH-1S (small) [70,71]. In our gels, the medium-sized NDH-1M complex was the most prominent (Fig. 5A, B). At least four different spots were identified as belonging to the NDH-1M complexes, of which we identified the NdhH, NdhK and NdhI subunits. One spot possibly containing the NdhJ subunit could not be unequivocally identified due to contamination from the nearby NdhK protein spot. We did not observe the NDH-1S complex. The NDH-1L complex was only barely distinguishable, and we could not discern the subunits in this complex.

In cyanobacteria, NDH-1 is known to participate in respiratory electron transfer, as well as cyclic electron transfer around PSI [72–75]. It displays a remarkable functional and structural plasticity, and is known to have different subunit composition depending on growth conditions [36,74]. Due to its promiscuity in electron transfer partners, the NDH-1 complex probably has an important role in cyanobacterial acclimation to varying environmental conditions [76–78]. It has been suggested that the NDH-1L complex is essential for respiration and photoheterotrophic growth [79]. Only when *Synechocystis* PCC 6803 is grown under carbon-limiting conditions, does the NDH-1M complex accumulate in any larger quantities [70]. In a CO_2 enriched atmosphere on the other hand, the NDH-1L complex dominated over the lighter NDH-1M complex. Since we cultured our strains under CO_2-enriched atmosphere, we did not expect the amounts of NDH-1L complexes to be so much lower than the NDH-1M complexes. This difference between the heterocysts of *Nostoc punctiforme* and *Synechocystis* PCC 6803 suggests that the occurrence of the different NDH-1 complexes depends on other factors. Interestingly, mutant strains of *Synechocystis* PCC 6803 lacking the ability to form NDH-1L complexes, displayed rates of re-reduction of P^+_{700} that were close to wild-type levels, suggesting the NDH-1M complex could be able to support PSI-based cyclic electron transport [70]. In heterocysts, PSI is assumed to mainly participate in electron transport involving respiratory enzymes, such as the Cytochrome-b_6/*f* and NDH-1 complexes. The present results suggest that it is possible that the NDH-1M complex might be critical for supporting this function.

3.7. Photosystem II electron transfer

The lack of oxygen evolution and variable fluorescence from PSII in isolated heterocysts, has led to the conventional assumption that PSII is completely inactive if not absent in heterocysts [10–13,80]. A few attempts of measuring electron transport involving PSII have been made on isolated heterocysts and/or whole homogenates from ruptured heterocysts [13,28,81]. Light-induced reduction of artificial electron acceptors has been measured in broken heterocysts from *Anabaena cylindrica*, but the activity was ascribed to a reaction with Photosystem I [81].

We measured the light-driven electron transport through PSII in thylakoid membranes from both vegetative cells and heterocysts. To assess the PSII electron transport activity, the light-driven reduction of the electron acceptor DCPIP, which accepts electrons at the Q_B-binding site in PSII, was followed spectrophotometrically. The results are shown in Table 2. Reduction of DCPIP was obtained in vegetative cells with either water as electron donor, or by using the exogenous electron donor DPC, which donates electrons to the redox active tyrosine residue on the D1 protein, Tyrosine$_Z$ (Y_Z). In heterocysts, we detected no activity from the water oxidizing complex, i.e. the electron

Table 2
Electron transfer measured in isolated thylakoid membranes

	Photo-induced DCPIP reduction μmol DCPIP (mg Chl-*a*)$^{-1}$ h^{-1}			
	H_2O as electron donor	DPC+H_2O as electron donor	DPC+H_2O +DCMU	Fraction of active PSII[a]
Filaments	27±5	34±7	0	0.80
Heterocysts	0	3.9±0.6	0	0
Contamination control[b]	2.4	3.7	0	0.65

[a] The percentage of Photosystem II centres active in water oxidation was calculated as the ratio between DCPIP reduction with only H_2O as electron donor, and the total DCPIP reduction after addition of the extraneous electron donor DPC.

[b] A 10% contamination from vegetative cell thylakoids was emulated by measuring the activity in vegetative thylakoids, at a concentration corresponding to 10% of that in the measurements made with the heterocyst membranes. In the table we have corrected the measured activity to the chlorophyll content in the sample of heterocyst membranes (see text for details).

transport from water to DCPIP was close to zero. With the exogenous electron donor DPC however, we found a reduction rate of 4 μmol DCPIP reduced mg^{-1} (Chl-*a*) h^{-1} (Table 2). On a Chl-*a* basis, this corresponds to ca 13% of the reduction rate found in thylakoid membranes from vegetative cells, in the presence of DPC. We also did the measurement with the inhibitor DCMU, which specifically blocks electron donation to the Q_B-binding site. In the presence of DCMU all of the observable DCPIP reduction activity was lost, clearly demonstrating that all observed activity occurred in PSII.

To determine if the observed electron transfer activity in the heterocyst preparation could be due to contamination of membranes from vegetative cells, we made additional measurements of electron transfer in vegetative thylakoid membranes. We performed the measurements at chlorophyll concentrations emulating contamination of 1%, 5%, 10% and 20% of vegetative thylakoids, based on the Chl-*a* concentrations used in the heterocyst measurements. The measured electron transfer activities were corrected at each of the different concentrations, to the total Chl-*a* concentration in the heterocyst membranes. We found that the sample corresponding to a 10% contamination of vegetative cell thylakoids, showed the same electron transfer activity as in the heterocyst samples, after addition of the exogenous electron donor DPC (Table 2). On the other hand, when we did the measurement without any addition of DPC, we obtained an electron transfer activity of as much as 65% of that in the presence of DPC, due to the water-splitting activity of PSII in the vegetative cell thylakoids. In contrast, no such activity could be detected in our heterocyst membranes in the absence of DPC. Therefore, although a 10% contamination of vegetative cell thylakoids would result in the obtained electron transfer activity in heterocysts, we would have detected the normal electron transfer from water to DCPIP from such a large fraction of thylakoid membranes from vegetative cells, with ease. Since no activity was detected in heterocyst thylakoids in the absence of DPC, we conclude that the observed PSII activity was intrinsic of the heterocyst membranes and not due to contamination.

We conclude that heterocyst thylakoid membranes show light-induced electron transport through PSII from DPC to DCPIP, corresponding to 13% of the activity in vegetative cells, on a total Chl-*a* basis.

The PSII complexes in the heterocyst thylakoid membranes are capable of light-induced electron transport, and are thus active in all respects except for the water oxidizing complex. To investigate if this could be due to a lack of manganese, the total amount of Mn in heterocysts was determined by EPR spectroscopy. It was found that the amount of Mn ions in heterocysts was 27% of that in the vegetative cells of *Nostoc punctiforme*, per Chl-*a*. Given that the PSII/PSI ratio is considerably lower in the heterocysts, the amount of available Mn per Chl-*a* seems quite sufficient for maintaining the water oxidizing complex. Therefore, the heterocysts apparently contain the minimum requirements necessary for performing water oxidation. However, this seems not to be the case since we did not observe any oxygen evolution in isolated heterocyst thylakoids.

The light-driven assembly of the water oxidizing complex, termed photoactivation, takes place in all cyanobacteria and plants without aid from any maturation systems [76]. During photoactivation, the water oxidizing complex is assembled stepwise via oxidation of each Mn ion, by the photo-induced charge separation in the reaction centre. Photoactivation requires a functional electron transfer pathway through assembled core PSII complexes, containing the D1, D2, CP43, CP47 and Cytochrome-b_{559} subunits, and the availability of Mn (II) and Ca(II) ions [82–84]. We have demonstrated the presence of such core PSII complexes in the heterocyst thylakoid membranes, but not in the cell wall-associated membranes (above). It is therefore conceivable that photoactivation could take place in heterocysts.

A possible explanation for the lack of photoactivated PSII centres, is a slow down of electron transfer on the electron acceptor side of PSII: At the onset of photoactivation, before the Mn complex is fully assembled, the electron transfer from PSII to the plastoquinone pool is slow. This is because the redox potential of the primary electron acceptor Q_A is higher in the absence of an active Mn complex, than in the fully active enzyme, making the Q_A a slow electron donor to plastoquinone (reviewed in [85]). Before the enzyme contains a functional water oxidation complex, the first charge separation reactions are able to take place with the assistance of auxiliary electron donors such as the redox active tyrosine residue on the D2 protein (denoted Y_D) as well as the Cytochrome-b_{559} [86]. The rate of electron transfer from Q_A to the plastoquinone pool subsequently becomes faster [86,87], until it is fast enough for efficient photoactivation.

In heterocysts, the plastoquinone pool is most likely engaged in cyclic electron transport around PSI, and it is unlikely that oxidized plastoquinone will build up in enough concentrations that it can reach PSII and support photoactivation. Charge separation in PSII will then result in charge recombination, and mainly involve the auxiliary electron donors (Y_D and Cyt-b_{559}, see above). Therefore, under illumination PSII will have little chance to undergo full photoactivation. However, after a long period of darkness, the supply of electron sources from the vegetative cells might run sparse. In that case the plastoquinone pool could become oxidized enough to enable photoactivation of PSII during the first moments when the light returns.

A possible explanation for the existence of PSII complexes in heterocysts, is therefore that it might function as a 'back-up' system for utilizing water as a provisional electron source, either during heterocyst development, or after periods of darkness when supply of carbohydrates from the vegetative cells runs low.

Acknowledgements

The authors would like to thank Professor Stenbjörn Styring for stimulating discussions. Mr. Erik Nagel is acknowledged posthumously for initial work on heterocyst isolation. Mr. Stefan Gunnarsson is acknowledged for help with the confocal microscope images.

This work was supported by grants from The Swedish Energy Agency, The Knut and Alice Wallenberg Foundation, The Swedish Research Council, the EU NEST project SOLAR-H2 (Contract no. 212508), The Nordic Energy Research project BioH2, The Academy of Finland, The Carl Trygger Foundation, and the Magnus Bergvall Foundation.

References

[1] J.C. Meeks, E.L. Campbell, M.L. Summers, F.C. Wong, Cellular differentiation in the cyanobacterium *Nostoc punctiforme*, Arch. Microbiol. 178 (2002) 395–403.
[2] P. Lindblad, C.A. Atkins, J.S. Pate, N_2-fixation by freshly isolated *Nostoc* from coralloid roots of the cycad *Macrozamia riedlei* (Fisch. ex Gaud.), Plant Physiol. 95 (1991) 753–759.
[3] A. Martel, E. Jansson, G. Garcia-Reina, P. Lindblad, Ornithine cycle in *Nostoc* PCC 73102. Arginase, OCT and arginine deiminase, and the effects of addition of external arginine, ornithine, or citrulline, Arch. Microbiol. 159 (1993) 506–511.
[4] J.C. Meeks, J. Elhai, T. Thiel, M. Potts, F. Larimer, J. Lamerdin, P. Predki, R. Atlas, An overview of the genome of *Nostoc punctiforme*, a multicellular, symbiotic cyanobacterium, Photosynth. Res. 70 (2001) 85–106.
[5] J.C. Meeks, J. Elhai, Regulation of cellular differentiation in filamentous cyanobacteria in free-living and plant-associated symbiotic growth states, Microbiol. Mol. Biol. Rev. 66 (2002) 94–121.
[6] R. Rippka, A. Neilson, R. Kunisawa, G. Cohen-Bazire, Nitrogen fixation by unicellular blue-green algae, Arch. Mikrobiol. 76 (1971) 341–348.
[7] I. Berman-Frank, P. Lundgren, P. Falkowski, Nitrogen fixation and photosynthetic oxygen evolution in cyanobacteria, Res. Microbiol. 154 (2003) 157–164.
[8] D.C. Rees, J.B. Howard, Nitrogenase: standing at the crossroads, Curr. Opin. Chem. Biol. 4 (2000) 559–566.
[9] C.P. Wolk, A. Ernst, J. Elhai, Heterocyst metabolism and development, in: D.A. Bryant (Ed.), Advances in Photosynthesis, Vol. 1, The molecular biology of cyanobacteria, Springer (Kluwer Academic Publishers), Dordrecht, 1994, pp. 769–823.
[10] P. Fay, Oxygen relations of nitrogen fixation in cyanobacteria, Microbiol. Rev. 56 (1992) 340–373.
[11] W. Zhao, Z. Ye, J. Zhao, RbrA, a cyanobacterial rubrerythrin, functions as a FNR-dependent peroxidase in heterocysts in protection of nitrogenase from damage by hydrogen peroxide in *Anabaena* sp. PCC 7120, Mol. Microbiol. 66 (2007) 1219–1230.

[12] J. Thomas, Relationship between age of culture and occurrence of pigments of Photosystem II of photosynthesis in heterocysts of a blue-green alga, J. Bacteriol. 110 (1972) 92–95.
[13] E. Tel-Or, W.D.P. Stewart, Photosynthetic components and activities of nitrogen-fixing heterocysts of *Anabaena cylindrica*, P. Roy. Soc. B 198 (1977) 61–86.
[14] T. Thiel, T. Hartnett, H.B. Pakrasi, Examination of Photosystem II in heterocysts of the cyanobacterium *Nostoc*. sp. ATCC 29150, in: M. Baltscheffsky (Ed.), Current research in photosynthesis, vol. 1, Kluwer academic publishers, The Netherlands, 1990, pp. 291–294.
[15] K. Black, B. Osborne, An assessment of photosynthetic downregulation in cyanobacteria from the *Gunnera-Nostoc* symbiosis, New Phytol. 162 (2004) 125–132.
[16] A.E. Walsby, The permeability of heterocysts to the gases nitrogen and oxygen, P. Roy. Soc. B-Biol. Sci. 226 (1985) 345–366.
[17] M.A. Murry, C.P. Wolk, Evidence that the barrier to the penetration of oxygen into heterocysts depends upon 2 layers of the cell-envelope, Arch. Microbiol. 151 (1989) 469–474.
[18] R.B. Peterson, R.H. Burris, Properties of heterocysts isolated with colloidal silica, Arch. Microbiol. 108 (1976) 35–40.
[19] D. Pils, C. Wilken, A. Valladares, E. Flores, G. Schmetterer, Respiratory terminal oxidases in the facultative chemoheterotrophic and dinitrogen fixing cyanobacterium *Anabaena variabilis* strain ATCC 29413: characterization of the *cox2* locus, BBA-Bioenergetics 1659 (2004) 32–45.
[20] A. Valladares, I. Maldener, A.M. Muro-Pastor, E. Flores, A. Herrero, Heterocyst development and diazotrophic metabolism in terminal respiratory oxidase mutants of the cyanobacterium *Anabaena* sp. strain PCC 7120, J. Bacteriol. 189 (2007) 4425–4430.
[21] M.L. Summers, J.G. Wallis, E.L. Campbell, J.C. Meeks, Genetic evidence of a major role for glucose-6-phosphate dehydrogenase in nitrogen fixation and dark heterotrophic growth of the cyanobacterium *Nostoc* sp. strain ATCC 29133, J. Bacteriol. 177 (1995) 6184–6194.
[22] H. Böhme, Regulation of nitrogen fixation in heterocyst forming cyanobacteria, Trends Plant Sci. 3 (1998) 346–351.
[23] A.C. Cumino, C. Marcozzi, R. Barreiro, G.L. Salerno, Carbon cycling in *Anabaena* sp. PCC 7120. Sucrose synthesis in the heterocysts and possible role in nitrogen fixation, Plant Physiol. 143 (2007) 1385–1397.
[24] H. Böhme, B. Schrautemeier, Regulation of electron flow to nitrogenase in a cell-free system from heterocysts of *Anabaena variabilis*, BBA-Bioenergetics 891 (1987) 115–120.
[25] B. Masepohl, K. Scholisch, K. Gorlitz, C. Kutzki, H. Böhme, The heterocyst-specific fdxH gene product of the cyanobacterium *Anabaena* sp. PCC 7120 is important but not essential for nitrogen fixation, Mol. Gen. Genet. 253 (1997) 770–776.
[26] P. Razquin, M.F. Fillat, S. Schmitz, O. Stricker, H. Böhme, C. Gomez-Moreno, M.L. Peleato, Expression of ferredoxin-NADP+ reductase in heterocysts from *Anabaena* sp. Biochem. J. 316 (1996) 157–160.
[27] S.Y. Ow, T. Cardona, A. Taton, A. Magnuson, P. Lindblad, K. Stensjö, P.C. Wright, Quantitative shotgun proteomics of enriched heterocysts from *Nostoc* sp. PCC 7120 using 8-plex isobaric peptide tags, J. Proteome Res. 7 (2008) 615–626.
[28] H. Almon, H. Böhme, Components and activity of the photosynthetic electron transport of intact heterocysts isolated from the blue-green alga *Nostoc muscorum*, BBA-Bioenergetics 592 (1980) 113–120.
[29] J.P. Houchins, G. Hind, Concentration and function of membrane-bound cytochromes in cyanobacterial heterocysts, Plant Physiol. 76 (1984) 456–460.
[30] S. Janaki, C.P. Wolk, Synthesis of nitrogenase by isolated heterocysts, BBA-Gene Struc. Expr. 696 (1982) 187–192.
[31] E. Gantt, Supramolecular membrane organization, in: D.A. Bryant (Ed.), Advances in Photosynthesis, Vol. 1, The molecular biology of cyanobacteria, Springer (Kluwer academic publishers), Dordrecht, 1994, pp. 119–138.
[32] G. Schmetterer, Cyanobacterial respiration, in: D.A. Bryant (Ed.), Advances in Photosynthesis, Vol. 1, The molecular biology of cyanobacteria, Kluwer academic publishers, Dordrecht, 1994, pp. 409–435.
[33] N. Lang, P. Fay, The heterocysts of blue-green algae II. Details of ultrastructure, P. Roy. Soc. B 178 (1971) 193–203.
[34] D.C. Anderson, E.L. Campbell, J.C. Meeks, A soluble 3D LC/MS/MS proteome of the filamentous cyanobacterium *Nostoc punctiforme*, J. Proteome Res. 5 (2006) 3096–3104.
[35] S.Y. Ow, J. Noirel, T. Cardona, A. Taton, P. Lindblad, K. Stensjö, P.C. Wright, Quantitative overview of N_2 Fixation in *Nostoc punctiforme* ATCC 29133 through cellular enrichments and iTRAQ shotgun proteomics, J. Proteome Res. 8 (2009) 187–198.
[36] M. Herranen, N. Battchikova, P. Zhang, A. Graf, S. Sirpiö, V. Paakarinen, E.M. Aro, Towards functional proteomics of membrane protein complexes in *Synechocystis* sp. PCC 6803, Plant Physiol. 134 (2004) 470–481.
[37] R. Srivastava, T. Pisareva, B. Norling, Proteomic studies of the thylakoid membrane of *Synechocystis* sp PCC 6803, Proteomics 5 (2005) 4905–4916.
[38] T. Cardona, N. Battchikova, Å. Agervald, P. Zhang, E. Nagel, E.-M. Aro, S. Styring, P. Lindblad, A. Magnuson, Isolation and characterization of thylakoid membranes from the filamentous cyanobacterium *Nostoc punctiforme*, Physiol. Plant. 131 (2007) 622–634.
[39] R.L. Smith, C. van Baalen, F.R. Tabita, Isolation of metabolically active heterocysts from cyanobacteria, Methods in Enzymology, Vol. 167, Cyanobacteria, Elsevier, 1988, 490–495.
[40] J. Meeks, R. Castenholtz, Growth and photosynthesis in an extreme thermophile, *Synechococcus lividus* (Cyanophyta), Arch. Mikrobiol. 78 (1971) 25–41.
[41] C. Jegerschöld, I. Virgin, S. Styring, Light-dependent degradation of the D1 protein in Photosystem II is accelerated after inhibition of the water-splitting reaction, Biochemistry 29 (1990) 6179–6186 -US.
[42] U.K. Laemmli, Cleavage of structural proteins during the assembly of the head of bacteriophage T4, Nature 227 (1970) 680–685.
[43] H. Blum, H. Beier, H.J. Gross, Improved silver staining of plant proteins, RNA and DNA in polyacrylamide gels, Electrophoresis 8 (1987) 93–99.
[44] A. Shevchenko, M. Wilm, O. Vorm, M. Mann, Mass spectrometric sequencing of proteins from silver stained polyacrylamide gels, Anal. Chem. 68 (1996) 850–858.
[45] D. Liu, J.W. Golden, *hetL* overexpression stimulates heterocyst formation in *Anabaena* sp. strain PCC 7120, J. Bacteriol. 184 (2002) 6873–6881.
[46] J. Thomas, Absence of the pigments of Photosystem II of photosynthesis in heterocysts of a blue-green alga, Nature 228 (1970) 181–183.
[47] K. Baier, H. Lehmann, D.P. Stephan, W. Lockau, NblA is essential for phycobilisome degradation in *Anabaena* sp strain PCC 7120 but not for development of functional heterocysts, Microbiology 150 (2004) 2739–2749 (-SGM).
[48] E. Wolf, A. Schussler, Phycobiliprotein fluorescence of *Nostoc punctiforme* changes during the life cycle and chromatic adaptation: characterization by spectral confocal laser scanning microscopy and spectral unmixing, Plant Cell Environ. 28 (2005) 480–491.
[49] P. Jordan, P. Fromme, H.T. Witt, O. Klukas, W. Saenger, N. Krauss, Three-dimensional structure of cyanobacterial Photosystem I at 2.5 Ångstrom resolution, Nature 411 (2001) 909–917.
[50] R.B. Peterson, E.R. Shaw, E. Dolan, B. Ke, A photochemically active heterocyst preparation from *Anabaena variabilis*, Photobiochem. Photobiophys. 2 (1981) 79–84.
[51] D. Fork, P. Mohanty, Fluorescence and other characteristics of blue-green algae (cyanobacteria), red algae and cryptomonads, in: J. Govindjee, Amesz, D.C. Fork (Eds.), Light Emission by Plants and Bacteria, Academic Press, Orlando, 1986, pp. 451–490.
[52] C.W. Mullineaux, Phycobilisome-reaction centre interaction in cyanobacteria, Photosynth. Res. 95 (2008) 175–182.
[53] M.D. McConnell, R. Koop, S. Vasilev, D. Bruce, Regulation of the distribution of chlorophyll and phycobilin-absorbed excitation energy in cyanobacteria. A structure-based model for the light state transition, Plant Physiol. 130 (2002) 1201–1212.
[54] R. Zhang, H. Li, J. Xie, J. Zhao, Estimation of relative contribution of "mobile phycobilisome" and "energy spillover" in the light–dark induced state transition in *Spirulina platensis*, Photosynth. Res. 94 (2007) 315–320.
[55] X. Su, P.G. Fraenkel, L. Bogorad, Excitation energy transfer from phycocyanin to chlorophyll in an apcA-defective mutant of *Synechocystis* sp. PCC 6803, J. Biol. Chem. 267 (1992) 22944–22950.
[56] K. Kondo, Y. Ochiai, M. Katayama, M. Ikeuchi, The membrane-associated CpcG2-phycobilisome in *Synechocystis*: a new Photosystem I antenna, Plant Physiol. 144 (2007) 1200–1210.
[57] L. Curatti, L. Giarrocco, G.L. Salerno, Sucrose synthase and Rubisco expression is similarly regulated by the nitrogen source in the nitrogen-fixing cyanobacterium *Anabaena* sp. Planta 223 (2006) 891–900.
[58] E.B. Braun-Howland, S.A. Nierzwicki-Bauer, Occurrence of the 32-kDa QB-binding protein of Photosystem-II in vegetative cells, heterocysts and akinetes, of *Azolla caroliniana* cyanobionts, Planta 180 (1990) 361–371.
[59] E-M. Aro, I. Virgin, B. Andersson, Photoinhibition of photosystem II. Inactivation, protein damage and turnover, BBA-Bioenergetics 1143 (1993) 113–134.
[60] B. Andersson, E.-M. Aro, Photodamage and D1 protein turnover in Photosystem II, in: E.-M. Aro, B. Andersson (Eds.), Regulation of Photosynthesis, Kluwer Academic Publishers, The Netherlands, 2001, pp. 377–393.
[61] P.J. Nixon, M. Barker, M. Boehm, R. de Vries, J. Komenda, FtsH-mediated repair of the photosystem II complex in response to light stress, J. Exp. Bot. 56 (2004) 357–363.
[62] W. Lockau, R.B. Peterson, C.P. Wolk, C.H. Burris, Modes of reduction of nitrogenase in heterocysts isolated from *Anabaena* species, BBA-Bioenergetics 502 (1978) 298–308.
[63] K. Stensjö, S.Y. Ow, M.E. Barrios-Llerena, P. Lindblad, P.C. Wright, An iTRAQ-based quantitative analysis to elaborate the proteomic response of *Nostoc* sp. PCC 7120 under N_2 Fixing Conditions, J. Proteome Res. 6 (2007) 621–635.
[64] Z. Adam, A. Zaltsman, G. Sinvany-Villalobo, W. Sakamoto, FtsH proteases in chloroplasts and cyanobacteria, Physiol. Plant. 123 (2004) 386–390.
[65] N.H. Mann, N. Novac, C.W. Mullineaux, J. Newman, S. Bailey, C. Robinson, Involvement of an FtsH homologue in the assembly of functional Photosystem I in the cyanobacterium *Synechocystis* sp. PCC 6803, FEBS Lett. 479 (2000) 72–77.
[66] N. Bukhov, R. Carpentier, Alternative Photosystem I-driven electron transport routes: mechanisms and functions, Photosynth. Res. 82 (2004) 17–33.
[67] D.C. Fork, S.K. Herbert, Electron transport and photophosphorylation by Photosystem I in vivo in plants and cyanobacteria, Photosynth. Res. 36 (1993) 149–168.
[68] J.J. Van Thor, R. Jeanjean, M. Havaux, K.A. Sjollema, F. Joset, K.J. Hellingwerf, H.C.P. Matthijs, Salt shock-inducible Photosystem I cyclic electron transfer in *Synechocystis* PCC 6803 relies on binding of ferredoxin: NADP(+) reductase to the thylakoid membranes via its CpcD phycobilisome-linker homologous N-terminal domain, BBA-Bioenergetics 1457 (2000) 129–144.
[69] N. Battchikova, E.-M. Aro, Cyanobacterial NDH-1 complexes: multiplicity in function and subunit composition, Physiol. Plant. 131 (2007) 22–32.
[70] P. Zhang, N. Battchikova, T. Jansen, J. Appel, T. Ogawa, E.-M. Aro, Expression and functional roles of the two distinct NdhD3/NdhF3/CupA/Sll1735 in *Synechocystis* sp. PCC 6803, Plant Cell 16 (2004) 3326–3340.
[71] N. Battchikova, P. Zhang, S. Rudd, T. Ogawa, E.-M. Aro, Identification of NdhL and Ssl1690 (NdhO) in NDH-1L and NDH-1M complexes of *Synechocystis* sp. PCC 6803, J. Biol. Chem. 280 (2005) 2587–2595.
[72] H. Mi, T. Endo, U. Schreiber, T. Ogawa, K. Asada, Electron donation from cyclic and respiratory flows to the photosynthetic intersystem chain is mediated by pyridine nucleotide dehydrogenase in the cyanobacterium *Synechocystis* PCC 6803, Plant Cell Physiol. 33 (1992) 1233–1237.

[73] T. Ogawa, A gene homologous to the subunit-2 gene of NADH dehydrogenase is essential to inorganic carbon transport of *Synechocystis* PCC 6803, Proc. Natl. Acad. Sci. U. S. A. 88 (1991) 4275–4279.
[74] G. Peltier, L. Cournac, Chlororespiration, Annu. Rev. Plant Biol. 53 (2002) 523–550.
[75] T. Ogawa, H. Mi, Cyanobacterial NADPH dehydrogenase complexes, Photosynth. Res. 93 (2007) 69–77.
[76] R.M. Figge, C. Cassier-Chauvat, F. Chauvat, R. Cerff, Characterization and analysis of an NAD(P)H dehydrogenase transcriptional regulator critical for the survival of cyanobacteria facing inorganic carbon starvation and osmotic stress, Mol. Microbiol. 39 (2001) 455–468.
[77] T. Hibino, B.H. Lee, A.K. Rai, H. Ishikawa, H. Kojima, M. Tawada, H. Shimoyama, T. Takabe, Salt enhances Photosystem I content and cyclic electron flow via NAD(P)H dehydrogenase in the halotolerant cyanobacterium *Aphanothece halophytica*, Aust. J. Plant Phys. 23 (1996) 321–330.
[78] Y. Tanaka, S. Katada, H. Ishikawa, T. Ogawa, T. Takabe, Electron flow from NAD(P)H dehydrogenase to Photosystem I is required for adaptation to salt shock in the cyanobacterium *Synechocystis* sp. PCC 6803, Plant Cell Physiol. 38 (1997) 1311–1318.
[79] H. Ohkawa, H.B. Pakrasi, T. Ogawa, Two types of functionally distinct NAD(P)H dehydrogenases in *Synechocystis* sp. strain PCC 6803, J. Biol. Chem. 275 (2000) 31630–31634.
[80] C.P. Wolk, Heterocysts, in: N.G. Carr, B.A. Whitton (Eds.), The Biology of Cyanobacteria, Blackwell scientific, Oxford, 1982, pp. 359–386.
[81] M. Donze, A.J.P. Raat, H.J. van Gorkom, Supply of ATP and reductant to nitrogenase in blue-green algae *Anabaena cylindrica*, Plant. Sci. Lett. 3 (1974) 35–41.
[82] N. Tamura, G.M. Cheniae, Photoactivation of the water-oxidizing complex in Photosystem II membranes depleted of Mn and extrinsic proteins. 1. Biochemical and kinetic characterization, Biochim. Biophys. Acta 890 (1987) 179–194.
[83] N. Tamura, H. Kamachi, N. Hokari, H. Masumoto, H. Inoue, Photoactivation of the water-oxidizing complex in Photosystem II core complex depleted of functional Mn, Biochim. Biophys. Acta 1060 (1991) 51–58.
[84] C. Büchel, J. Barber, G. Ananyev, S. Eshaghi, R. Watt, C.G. Dismukes, Photoassembly of the manganese cluster and oxygen evolution from monomeric and dimeric CP47 reaction center Photosystem II complexes, Proc. Natl. Acad. Sci. 96 (1999) 14288–14293.
[85] F. Mamedov, S. Styring, Logistics in the life cycle of Photosystem II — lateral movement in the thylakoid membrane and activation of electron transfer, Physiol. Plant. 131 (2007) 328–336.
[86] A. Magnuson, M. Rova, F. Mamedov, P.-O. Fredriksson, S. Styring, The role of cytochrome b(559) and tyrosine(D) in protection against photoinhibition during in vivo photoactivation of Photosystem II, Biochim. Biophys. Acta 1411 (1999) 180–191.
[87] M. Rova, F. Mamedov, A. Magnuson, P.-O. Fredriksson, S. Styring, Coupled activation of the donor and the acceptor side of Photosystem II during photoactivation of the oxygen evolving cluster, Biochemistry 37 (1998) 11039–11045.